ISSN 1063-780X, Plasma Physics Reports, 2023, Vol. 49, No. 10, pp. 1151–1161. 

**STELLARATORS**

*In memory of A.V. Timofeev*

# Reflection of the Electromagnetic Wave from the Region of Electron Cyclotron Absorption in Thermonuclear Plasma

**E. D. Gospodchikov[a,*], P. A. Chuvakin[a], and A. G. Shalashov[a]**

[a] *Gaponov-Grekhov Institute of Applied Physics, Russian Academy of Sciences, Nizhny Novgorod, 603950, Russia*

**e-mail: egos@ipfran.ru*

Received July 1, 2023; revised July 21, 2023; accepted July 22, 2023

**Abstract**—A new approach to the problem of the passage of the extraordinary wave through the region of the electron–cyclotron resonance in inhomogeneous plasma was considered in the framework of the full set of Maxwell's equations, taking into account the effects of spatial dispersion and resonance dissipation. For the model one-dimensional geometry, field distributions were calculated in the vicinity of the cyclotron resonance at the second harmonic for the normal incidence of the extraordinary wave and the reflection, transmission, and absorption coefficients were found depending on the parameters of the resonance region. As a result, the fine effect of the reflection of electromagnetic radiation from the cyclotron resonance region in transparent plasma was described and the results were compared with the observations of this effect in the experiments on the microwave heating of the plasma at the L-2M stellarator.

**Keywords:** high-temperature plasma, electron-cyclotron resonance, second harmonic, full-wave simulations, quasielectrostatic waves

**DOI:** 10.1134/S1063780X23601128

## 1. INTRODUCTION

The theory of the interaction of electromagnetic radiation with inhomogeneous magnetoactive plasmas under cyclotron resonance conditions applied to the problems of the heating and diagnostics of the plasma was one of the branches of plasma physics to whose development Alexander Vladimirovich Timofeev made a significant deposition. The results of A.V. Timofeev's efforts were formulated most fully in his monograph [1]. This book, which was first published in 2000, remains relevant and in demand today. One of the important components of the theory are model problems, which allow one to obtain a clear and compact analytical and practical solution. Many such problems for waves propagating in the vicinity of plasma resonances were formulated and successfully solved by Alexander Vladmirovich and his students. In this article, we continue this line of work. Here, the known model problem of the reflection of the extraordinary wave incident on the region of the second harmonic electron cyclotron resonance (ECR) is considered [2–5]. We discuss a new approach to the solution of this problem, which is of significant practical interest for the interpretation of experiments on microwave heating of high-temperature plasmas in tokamaks and stellarators. A.V. Timofeev was one of the first to note the close connection, which appears in problems of this type, between the "fast" electromagnetic waves and the quasielectrostatic plasma oscillations in the vicinity of the cyclotron frequency and its harmonics [6], which, in hot plasma, obtain the characteristics of "slow" waves known as the electron or ion Bernstein waves [7]. More accurate than our predecessors' accounting for the linear interaction between the electromagnetic and Bernstein waves allowed us to progress toward the solution of our particular problem.

The propagation and resonance absorption of microwave radiation in the hot plasma in large magnetic traps has been long and successfully simulated in the framework of geometric (ray) optics [8–11] or by using the more complicated asymptotic methods [12–15] based on one of the formulations of the short-wave approximation for the Maxwell's equations in the smoothly inhomogeneous (on the scale of the wavelength) plasma (the Wentzel–Kramers–Brillouin (WKB) approximations). The general feature of such approximations is that they describe the wave beam that propagates in a selected direction (e.g., along the line-of-sight as far as the absorption region). In this case, the wave reflection can appear only as a result of refraction, i.e., the bending of the beam trace without changing its direction along the line of sight. This is the way, e.g., reflection occurs when the beam approaches the region of above-critical (nontransparent) plasma. However, the initial Maxwell's equations allow a second type of reflected wave, which propagates against the initial wave beam. In the smoothly inhomogeneous medium, one can assume that such waves propagate precisely along the track of the initial wave beam but in the opposite direction [16]. The processes of excitation of such counterpropagating waves, which, hereinafter, we will shorten to "reflection" are the object of study in this work.

Note that, in our terms, reflection is also possible in a transparent medium, if in it, a region where the WKB approximation is disrupted is present. In smoothly inhomogeneous plasma far from the region of resonance absorption, the direct and counterpropagating waves travel independently, and the counterpropagating waves have no source and are, therefore, ignored. However, in the resonance region, the characteristic scale of the inhomogeneity of the medium determined by the width of the cyclotron resonance can be comparable to or even shorter than the vacuum wavelength. Moreover, in this case, the imaginary part of the wave number is of the same order as its real part, and therefore, in the geometrical–optical description, the wave is completely absorbed over a distance that is shorter than one wavelength. All of this leads to a disruption of the WKB approximation and, from the theoretical viewpoint, it can lead to the appearance of significant reflection from the region of cyclotron resonance in the transparent (with a below-critical density) but absorbing plasma.

The power of radiation reflected from the ECR region in the case of plasma heating by the extraordinary wave at the second cyclotron harmonic was measured in experiments on the L-2M stellarator [17]. It was discovered that it was more than one order of magnitude higher than predicted by the elementary theory [2] based on the perturbation method (the next order of the WKB approximation). Note that, to the difference from some other experiments [18–20], in this case, the possible nonlinear nature of the microwave signal does not agree with the measurement results, in particular, due to the absence of the dependence of the reflection coefficient on the deposited power. The difficulty in interpreting the described experiments is caused by several factors:

(i) Describing the interaction between the direct and counterpropagating radiation requires one to look beyond the limits of the WKB approximation, i.e., to use the full set of Maxwell's equations, which can be simplified only due to the model of the medium's inhomogeneity;

(ii) In the vicinity of the cyclotron resonance, one needs to simultaneously account for the spatial dispersion and spatial inhomogeneity [21], and in this region, the counterpropagating electromagnetic waves not only interact with each other but also with the short-wave quasielectrostatic electron Bernstein waves [4, 5];

(iii) Since a fraction of the waves are strongly decaying or non-propagating, the problem is badly conditioned and requires a correct and extremely precise formulation of boundary conditions outside the resonance region (in the WKB region) [5, 22].

Factors (i) and (ii) were fully accounted for in independent works [5, 17], in both of which a theory of reflection of the extraordinary wave at the second cyclotron harmonic was proposed in the case of its strictly transverse propagation. At the same time, in [5], the problems connected to the loss of precision of the solution due to the "skinning" of Bernstein waves, i.e., factor (iii), were noted explicitly. In [17], the problems caused by the imprecise boundary conditions were not discussed, but they were present. In particular, the answer based on model [17] depends strongly on the exact location of the boundary conditions in the WKB region, which, in effect, adds one additional free parameter of nonphysical nature to the problem. In this work, we attempted to solve the problem with the boundary conditions using a formal approach that we called the "impedance method" [22, 23]. This is a variation of the more general invariant embedding method [24, 25] that is adapted to the search for the solution of Maxwell's equations in anisotropic gyrotropic media with spatial dispersion. At the same time, the physical model (the Maxwell's equations and the material relations) to a significant degree repeats the one considered in [5, 17]. It was only the approach to the formulation of the boundary conditions that we changed. The use of the impedance method allowed us, in particular, to resolve the problems described in [5], where the precision of the solution was decreased due to the presence of Bernstein waves.

As a result, for the model medium, we have numerically calculated the field distributions in the vicinity of the second harmonic of the cyclotron resonance when the extraordinary wave falls onto the resonance region normally to the external magnetic field. The dependences were calculated of the reflection, transmission, linear transformation, and absorption coefficients of the incident extraordinary wave on the parameters of the resonance region. The results were compared with the experimental results obtained at the L-2M stellarator.

## 2. EQUATIONS FOR THE ELECTRIC FIELD IN THE REGION OF SECOND-HARMONIC CYCLOTRON RESONANCE

As we have noted above, in general, the geometrical optics approximation adequately simulates the propagation of radiation in smoothly inhomogeneous magnetoactive plasmas. The region where this approximation is inapplicable is the vicinity of the region of the cyclotron resonance. The characteristic size $L_{\rm res}$ of this region is much smaller than the characteristic scales of the inhomogeneities of the plasma density $L_N$, the magnetic field $L_B$, and the electron temperature $L_T$. Thus, for a strictly normal propagation of the beam in a tokamak with a major radius $R$ and a minor radius $a$, the following scale hierarchy is true

$$L_{\rm res} \approx R/\mu = L_N \approx L_T \approx a < L_B \approx R, \quad (1)$$

where $\mu = mc^2/T_e$ is the ratio between the rest energy of electrons and their temperature. We consider the weakly relativistic case with $\mu \gg 1$. The inequalities (1) allow us to, first, limit ourselves to the plane-stratified model, second, consider the plasma density and electron temperature homogeneous in the interaction region, and, third, consider that the magnetic field changes by the linear law and that it is close to the resonance value. In addition, we will assume that the propagation direction of the wave incident on the resonance region (the $x$ coordinate) is perpendicular to the external magnetic field and the same as the direction of the gradient of the modulus of the external magnetic field. After making this set of assumptions, we use the explicit expression for the tensor of dielectric permittivity of the warm magnetoactive plasma in the vicinity of the second harmonic cyclotron resonance given in [21] and obtain the following closed set of Maxwell's equations for the electromagnetic field components $E_x$, $E_y$, and $H_z$

$$\frac{dE_y}{dx} = ik_0 H_z, \quad \frac{dH_z}{dx} = ik_0 D_y, \quad D_x = 0, \quad (2)$$

where

$$D_x = \varepsilon_\perp E_x + igE_y + \delta\hat{\varepsilon}[E_x - iE_y],$$
$$D_y = \varepsilon_\perp E_y - igE_x + i\delta\hat{\varepsilon}[E_x - iE_y],$$
$$\varepsilon_\perp = 1 - \frac{\omega_{\rm p}^2}{\omega^2 - \omega_{\rm c}^2}, \quad g = \frac{\omega_{\rm c}\omega_{\rm p}^2}{\omega(\omega^2 - \omega_{\rm c}^2)}, \quad (3)$$
$$\omega_{\rm p}^2 = \frac{4\pi e^2 N}{m}, \quad \omega_{\rm c}(x) = \frac{eB(x)}{mc}, \quad k_0 = \omega/c.$$

The correction to the dielectric response connected to the spatial dispersion is expressed by the differential operator

$$\delta\hat{\varepsilon}[\ldots] = \frac{1}{{\rm k}_0^2}\frac{d}{dx}\left(f(x)\frac{d}{dx}\ldots\right),$$
$$f(x) = \frac{1}{2}\frac{\omega_{\rm p}^2}{\omega_{\rm c}^2}F_{7/2}(\mu(1 - 2\omega_{\rm c}/\omega)), \quad (4)$$

where $F_{7/2}$ is the Dnestrovskii function [26]. Equations (2)–(4) describe the propagation, cyclotron absorption, and linear interaction of the extraordinary and Bernstein waves. The equations for the other field components that describe the extraordinary wave are split off in this geometry.

The above set of three equations that contain the second derivatives of the fields can be rewritten as a set of four linear equations of the first order

$$\frac{d}{dx}\boldsymbol{\Psi} = ik_0\hat{M}\boldsymbol{\Psi},$$
$$\boldsymbol{\Psi} = \begin{pmatrix} E_- \\ E_+ \\ \Phi \\ H_z \end{pmatrix}, \quad \hat{M} = \begin{pmatrix} 0 & 0 & -1/f & 0 \\ 0 & 0 & 1/f & 2 \\ -\varepsilon_-/2 & \varepsilon_+/2 & 0 & 0 \\ 0 & \varepsilon_+ & 0 & 0 \end{pmatrix}, \quad (5)$$

where $E_\pm = E_y \mp iE_x$ are the complex amplitudes of the waves that rotate in the ion and electron directions, respectively,

$$\Phi = \frac{if}{k_0}\frac{dE_-}{dx}, \quad \varepsilon_\pm = 1 - \frac{\omega_{\rm p}^2}{\omega(\omega \pm \omega_{\rm c})}. \quad (6)$$

Ostensibly, this result corresponds to the interaction in the resonance region of two types of waves (extraordinary and Bernstein) that propagate in the two possible directions (along and against the $x$ axis).

In the homogeneous medium, the set of equations (5) has a set of four particular solutions that correspond to normal plane waves

$$\boldsymbol{\Psi}^\pm_{\rm X,B} = \mathbf{e}^\pm_{\rm X,B}\exp(\pm in_{\rm X,B}k_0x). \quad (7)$$

Here, $n_{\rm X,B}$ are the refraction indices of the extraordinary (X) and Bernstein (B) waves, which are found as the eigenvalues of the $\hat{M}$ matrix from its biquadratic characteristic equation

$$n^4 - \left(\frac{\varepsilon_+ + \varepsilon_-}{2f} + 2\varepsilon_+\right)n^2 + \frac{\varepsilon_+\varepsilon_-}{f} = 0; \quad (8)$$

$\mathbf{e}^\pm_{\rm X,B}$ are the eigenvectors of the $\hat{M}$ matrix that, in our formulation of the problem, play the role of electromagnetic field polarization in normal waves; and the $\pm$ signs correspond to the two directions of propagation.

Figure 1 shows the dependence of the real and imaginary parts of the square of the refraction indices on the ratio of the "cold" electron gyrofrequency and the wave frequency (this ratio plays the role of the space coordinate). The figure clearly shows that beyond the resonance region, $n_{\rm B}^2 < 0$, i.e., the Bernstein wave becomes nonpropagating. Figures 1c–1e show the same dependence in more detail in the resonance region at several consecutively increasing values of the plasma density. It is seen that in this region, a mutual transformation of the electromagnetic and electrostatic waves is possible through the reconnection of the dispersion curves [3, 4]. Following along one dispersion curve, on the one side, far from the res-

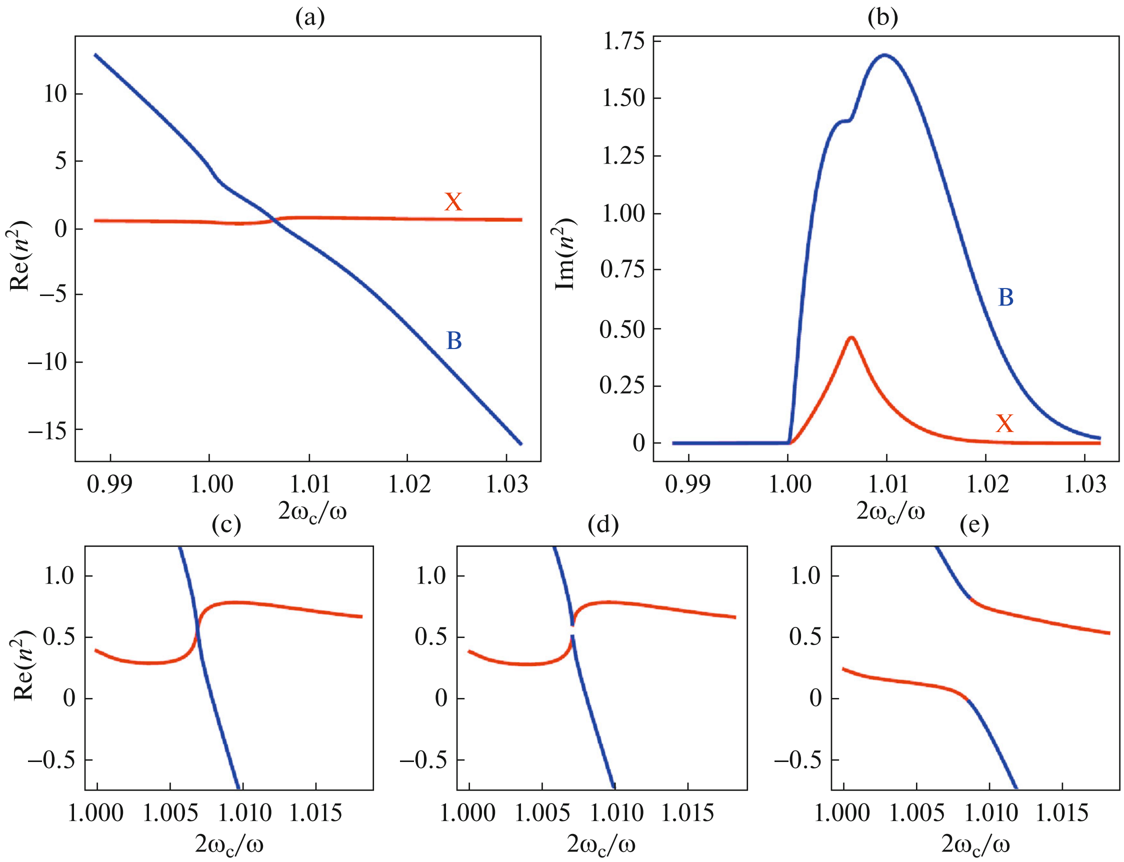


**Fig. 1.** The dependences of the (a) real and (b) imaginary parts of the square of the refraction index determined by the relation (8) on $2\omega_c/\omega$ for $\omega_p^2/\omega^2 = 0.25$. (c–e) The dependences of the real part of the refraction index inside the resonance region on $2\omega_c/\omega$ for (c) $\omega_p^2/\omega^2 = 0.281$, (d) $\omega_p^2/\omega^2 = 0.287$, and (e) $\omega_p^2/\omega^2 = 0.36$. The red curves correspond to the extraordinary (X) waves and the blue curves to Bernstein (B) waves. For all images, $T_e = 1$ keV.

onance, we have a wave with extraordinary polarization and on the other side, a Bernstein wave. Naturally, in the immediate region of the reconnection of the dispersion curves, it is impossible to consider the extraordinary and the Bernstein wave separately, and the normal waves in this region are a combination of bound Bernstein and extraordinary waves.

Solving the problem of the reflection of the incident extraordinary wave from the resonance region requires that we complement the equation set (5) by boundary conditions. Their physical formulation is the following: an extraordinary wave with the given (unit) amplitude falls onto the resonance region from the low magnetic field side ($2\omega_c < \omega$) and after the resonance region, at the high magnetic field side $2\omega_c > \omega$, only the transmitted extraordinary and Bernstein waves can exist (those that correspond to the "+" sign in Eq. (7)). Schematically, this is shown in Fig. 2. Note that the transmitted Bernstein wave decays exponentially in the region $2\omega_c > \omega$. To formulate the problem mathematically, we will assume that the medium is inhomogeneous only in the interval $(-x_0, +x_0)$. Outside of this interval, the medium is homogeneous, and there, the field is a combination of solutions (4). Consequently, our physical boundary

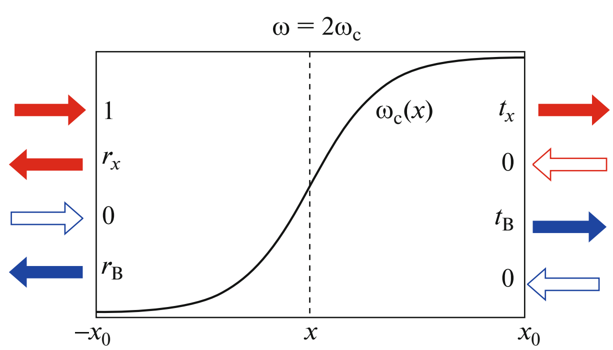


**Fig. 2.** Boundary conditions before $(-x_0)$ and after $(+x_0)$ in the interaction region $(\omega = 2\omega_c)$.

conditions will be formulated as follows: the sought-for vector field $\mathbf{\Psi}$ at the point $x = -x_0$ is

$$\mathbf{\Psi}(-x_0) = \mathbf{e}_X^+(-x_0) + r_X\mathbf{e}_X^-(-x_0) + r_B\mathbf{e}_B^-(-x_0), \quad (9)$$

while at the point $+x_0$ it is

$$\mathbf{\Psi}(+x_0) = t_X\mathbf{e}_X^+(+x_0) + t_B\mathbf{e}_B^+(+x_0). \quad (10)$$

Here, $r_{X,B}$ and $t_{X,B}$ are the unknown complex amplitudes of the extraordinary and Bernstein waves that were reflected from the layer and transmitted through it, respectively. The arguments $\pm x_0$ in the polarization vectors correspond to their calculation at the corresponding boundary of the inhomogeneity region. From a formal mathematical standpoint, the boundary conditions (9) and (10) consist of the coefficients before $\mathbf{e}_B^+(-x_0)$, $\mathbf{e}_X^-(+x_0)$, $\mathbf{e}_B^-(+x_0)$ being equal to zero and the coefficient before $\mathbf{e}_X^+(-x_0)$ being equal to unity. In such a formulation, the boundary conditions contain no unknown values and their number is exactly as many as are required for the single-value solution of Eqs. (5).

Although the complex amplitudes that were introduced completely characterize the reflection from the layer, in order to interpret the experimental results, it is more convenient to use the energy coefficients of reflection, transmission, and absorption. The reflection coefficient can be determined as the ratio between the energy flows of reflected waves (in both modes) and the flow of energy in the incident wave. In order to introduce the energy coefficients, let us write the law of the variation of the energy flow density, taking into account the resonance dissipation and the deposition of the spatial dispersion in the energy flow density [27]

$$\frac{dP_x}{dx} = -Q. \quad (11)$$

Here,

$$P_x = \frac{\omega}{16\pi}\mathrm{Re}(\Psi_1\Psi_4^* + \Psi_2\Psi_4^* - 2\Psi_1\Psi_3^{*}) \quad (12)$$

is the energy flow density expressed through the components of the $\mathbf{\Psi}$ vector; it consists of the corresponding component of the Pointing vector and the deposition of the spatial dispersion that is proportional to the derivative of the field phase, while

$$Q = -\frac{1}{8\pi}\frac{\mathrm{Im}\, f}{|f|^2}|\Psi_3|^2 \quad (13)$$

is the density of the microwave power absorbed under the cyclotron resonance conditions. Far from the resonance, $\mathrm{Im}f \to 0$, and we can ignore the absorption. At the same time, in the WKB region before the resonance, where the refraction indices are real, the energy flow density can be expressed as the sum of the partial densities of the energy flows in separate waves. If we introduce the energy flow densities that correspond to the extraordinary and Bernstein waves with unit amplitude as

$$N_{X,B} = P_x|_{\mathbf{\Psi}=\mathbf{e}_{X,B}^+}, \quad (14)$$

then, taking into account Eq. (8), we get the energy flow density at the layer boundary

$$P_x(-x_0) = N_X(-x_0)\left(1-|r_X|^2\right) - N_B(-x_0)|r_B|^2. \quad (15)$$

Behind the resonance region, where the refraction index for the Bernstein wave is purely imaginary, it is impossible to formally split the energy flow of the Bernstein wave into partial flows. However, it can be noted that, since beyond the resonance region, where the medium becomes homogeneous, only one Bernstein normal wave is present (and it decays exponentially at $x \to +\infty$), in this region, Bernstein waves do not carry energy. At the same time, the energy flow can be written as

$$P_x(+x_0) = N_X(+x_0)|t_X|^2. \quad (16)$$

As a result, we can introduce partial (separate for each mode) reflection and transmission coefficients for the wave intensity as follows

$$R_X = |r_X|^2, \quad T_X = \frac{N_X(+x_0)}{N_X(-x_0)}|t_X|^2,$$
$$R_B = \frac{N_B(-x_0)}{N_X(-x_0)}|r_B|^2, \quad T_B = 0. \quad (17)$$

By integrating Eq. (11), we find the absorption coefficient that reflects the fraction of absorbed power as

$$A = \int_{-\infty}^{+\infty} Q dx = 1 - R_X - R_B - T_X. \quad (18)$$

It was already noted that conditions (9) and (10) are the real boundary conditions for problem (5). The above considerations that the transmitted Bernstein wave decays exponentially beyond the resonance region and provides no deposition to the energy balance can lead to a temptation to assume that its amplitude is zero at the right-hand boundary. In this case, the solution to Eqs. (5) is substantially simplified, since instead of the boundary problem, one can solve the evolutionary Cauchy problem. Indeed, in Eq. (10), one can assume that the coefficient $t_B = 0$ before $\mathbf{e}_B^+(+x_0)$ and the coefficient $t_X$ before $\mathbf{e}_X^+(+x_0)$ is equal to any number, then calculate the problem backward to the point $x = -x_0$, expand $\mathbf{\Psi}(-x_0)$ over modes (7) and normalize the answer to the coefficient before $\mathbf{e}_X^+(-x_0)$. Due to the problem being linear, the coefficients before $\mathbf{e}_X^-(-x_0)$, $\mathbf{e}_B^-(-x_0)$, and $\mathbf{e}_X^+(+x_0)$ obtained in this way determine precisely the unknown coefficients of reflection and transmission in Eqs. (9) and (10) and, at the same time, the field vector $\mathbf{\Psi}(x)$ will be determined over the entire calculation interval.

This was the approach realized in [17], yet it generates an error.

Indeed, the solution $\mathbf{\Psi}(-x_0)$ found by the evolution method inevitably contains the projection to $\mathbf{e}_{\rm B}^{+}(-x_0)$. We will denote it as $a_{\rm B}$. Physically, this means that to obtain a zero Bernstein wave beyond the interaction region, we need a Bernstein wave with some strictly determined complex amplitude $a_{\rm B}$ to be present in the incident field, in addition to the extraordinary wave. This amplitude will be inversely proportional to the amplitude transmission coefficient of the Bernstein wave into the Bernstein wave, which, in turn, is exponentially small due to the "skinning" of the Bernstein wave along the $x$ axis. Therefore, the value $a_{\rm B}$ determined by integrating in the opposite direction from $x = +x_0$ to $-x_0$ can be arbitrarily large. Below, we present an alternative method of solving this problem, which guarantees a zero amplitude of the Bernstein wave before the interaction region ($a_{\rm B} = 0$) and is free from integrating over the exponentially growing solution.

## 3. IMPEDANCE METHOD OF SOLVING THE WAVE EQUATIONS

A more correct way of reducing the boundary problem to a set of Cauchy problems is the impedance method of solving the wave equations. This method in its general form was presented in [22, 23], yet we find it helpful to reiterate the main ideas of the method as they are applied to our problem.

We look for the solution of the set of equations (5) as an expansion over the normal waves that fulfill the following condition at the right-hand boundary $x = +x_0$

$$\begin{aligned}\mathbf{\Psi}(x) = \psi_{\rm X}^{+}(x)\,\mathbf{e}_{\rm X}^{+}(x_0) + \psi_{\rm X}^{-}(x)\,\mathbf{e}_{\rm X}^{-}(x_0)\\ + \psi_{\rm B}^{+}(x)\,\mathbf{e}_{\rm B}^{+}(x_0) + \psi_{\rm B}^{-}(x)\,\mathbf{e}_{\rm B}^{-}(x_0).\end{aligned} \quad (19)$$

The four coefficients $\psi_{\rm X,B}^{\pm}$ of this expansion are the new unknown functions that we use instead of the four components of the $\mathbf{\Psi}$ vector to determine the wave field. The set of linear equations for these coefficients, which is equivalent to the initial equations (2) is the following

$$\frac{d}{dx}\begin{pmatrix}\psi_{\rm X}^{+}\\ \psi_{\rm B}^{+}\\ \psi_{\rm X}^{-}\\ \psi_{\rm B}^{-}\end{pmatrix} = ik_0\hat{M}'\begin{pmatrix}\psi_{\rm X}^{+}\\ \psi_{\rm B}^{+}\\ \psi_{\rm X}^{-}\\ \psi_{\rm B}^{-}\end{pmatrix}, \quad (20)$$

where $\hat{M}' = \hat{U}^{-1}(x_0)\hat{M}(x)\hat{U}(x_0)$, $\hat{U}(x_0)$ is the transfer matrix to the basis of normal waves that correspond to the right-hand boundary, and the columns of the matrix are the eigenvectors $\mathbf{e}_{\rm X,B}^{\pm}(x_0)$. Let us separate in the $4 \times 4$ $\hat{M}'(x)$ matrix four $2 \times 2$ quadrants, which can be identified with some formal operators $\hat{t}^{\pm}$ and $\hat{r}^{\pm}$ in the two-dimensional space

$$\hat{M}'(x) = \begin{pmatrix}\hat{t}^{+} & \hat{r}^{-}\\ -\hat{r}^{+} & -\hat{t}^{-}\end{pmatrix}. \quad (21)$$

Equations (20) are then written as

$$\begin{cases}\dfrac{d}{dx}\begin{pmatrix}\psi_{\rm X}^{+}\\ \psi_{\rm B}^{+}\end{pmatrix} = ik_0\hat{t}^{+}\begin{pmatrix}\psi_{\rm X}^{+}\\ \psi_{\rm B}^{+}\end{pmatrix} + ik_0\hat{r}^{-}\begin{pmatrix}\psi_{\rm X}^{-}\\ \psi_{\rm B}^{-}\end{pmatrix},\\[2ex] \dfrac{d}{dx}\begin{pmatrix}\psi_{\rm X}^{-}\\ \psi_{\rm B}^{-}\end{pmatrix} = -ik_0\hat{r}^{+}\begin{pmatrix}\psi_{\rm X}^{+}\\ \psi_{\rm B}^{+}\end{pmatrix} - ik_0\hat{t}^{-}\begin{pmatrix}\psi_{\rm X}^{-}\\ \psi_{\rm B}^{-}\end{pmatrix}.\end{cases} \quad (22)$$

We introduce another matrix, $\hat{R}(x)$, as follows:

$$\begin{pmatrix}\psi_{\rm X}^{-}\\ \psi_{\rm B}^{-}\end{pmatrix} = \hat{R}\begin{pmatrix}\psi_{\rm X}^{+}\\ \psi_{\rm B}^{+}\end{pmatrix}. \quad (23)$$

This is a yet-unknown $2 \times 2$ matrix that connects the opposing modes, and therefore, it can be interpreted as the local operator of the reflection of the waves propagating in the "+" direction into the waves propagating in the "–" direction. After substituting Eq. (23) into Eq. (22), we obtain the following set of equations for the components of the reflection matrix and the "+" wave

$$\begin{cases}\dfrac{d}{dx}\hat{R} = -ik_0(\hat{R}\hat{r}^{-}\hat{R} + \hat{R}\hat{t}^{+} + \hat{t}^{-}\hat{R} + \hat{r}^{+}),\\[2ex] \dfrac{d}{dx}\begin{pmatrix}\psi_{\rm X}^{+}\\ \psi_{\rm B}^{+}\end{pmatrix} = ik_0(\hat{t}^{+} + \hat{r}^{-}\hat{R})\begin{pmatrix}\psi_{\rm X}^{+}\\ \psi_{\rm B}^{+}\end{pmatrix}.\end{cases} \quad (24)$$

The first of Eqs. (24) is an evolutionary nonlinear problem with a rudimentary initial condition at the right-hand boundary $\hat{R}(x_0) = 0$ (beyond the cyclotron region, there are no waves propagating from the $+\infty$ direction). This equation allows one to determine the distribution of $\hat{R}(x)$, which is a part of the second equation, over the entire calculation region,. At the same time, despite the integration being made in the opposite direction, from $x = +x_0$ to $-x_0$, the value $\hat{R}(x)$ remains limited throughout [22], eliminating the errors caused by the exponential decay of the Bernstein wave.

To write down the initial condition for the second equation in (24), it is sufficient to express the condition (9) before the cyclotron resonance region, which was formulated for the set of normal vectors at the left-hand boundary $\mathbf{e}^{\pm}_{X,B}(-x_0)$, through the coefficients of the $\mathbf{e}^{\pm}_{X,B}(+x_0)$ basis used in Eq. (19)

$$\hat{U}(x_0)\begin{pmatrix}\psi^+_X(-x_0)\\ \psi^+_B(-x_0)\\ \psi^-_X(-x_0)\\ \psi^-_B(-x_0)\end{pmatrix} = \hat{U}(-x_0)\begin{pmatrix}1\\0\\r_X\\r_B\end{pmatrix}, \quad (25)$$

where $\hat{U}(-x_0)$ is the transfer matrix to the basis of normal waves that correspond to the left-hand side boundary; and the columns of this matrix are the eigenvectors $\mathbf{e}^{\pm}_{X,B}(-x_0)$. After formally introducing the four $2 \times 2$ matrices $\hat{Q}_{ij}$ as

$$\begin{pmatrix}\hat{Q}_{11} & \hat{Q}_{12}\\ \hat{Q}_{21} & \hat{Q}_{22}\end{pmatrix} = \hat{U}^{-1}(-x_0)\hat{U}(x_0), \quad (26)$$

and taking into account that

$$\begin{pmatrix}\psi^-_X(-x_0)\\ \psi^-_B(-x_0)\end{pmatrix} = \hat{R}(-x_0)\begin{pmatrix}\psi^+_X(-x_0)\\ \psi^+_B(-x_0)\end{pmatrix}, \quad (27)$$

we can obtain the “solution” of the matrix relation (25) in the form of the explicit expression for the field at the left-hand boundary

$$\begin{pmatrix}\psi^+_X(-x_0)\\ \psi^+_B(-x_0)\end{pmatrix} = \left(\hat{Q}_{11} + \hat{Q}_{12}\hat{R}(-x_0)\right)^{-1}\begin{pmatrix}1\\0\end{pmatrix} \quad (28)$$

and the amplitude reflection coefficients

$$\begin{pmatrix}r_X\\ r_B\end{pmatrix} = \left(\hat{Q}_{12}\hat{R}(-x_0) + \hat{Q}_{21}\right)\left(\hat{Q}_{11} + \hat{Q}_{12}\hat{R}(-x_0)\right)^{-1}\begin{pmatrix}1\\0\end{pmatrix}. \quad (29)$$

The equality (28) determines the initial condition for the second equation in the set (24). The equality (29) allows one to recover the amplitudes of the reflected waves. Note that for this, it is sufficient to find the solution of the first equation in (24) with the initial condition $\hat{R}(x_0) = 0$.

By integrating the second equation of the set (24) as an evolutionary problem with initial conditions (28) at the left-hand boundary, we find $\psi^+_{X,B}(x)$ in the entire calculation space and, in particular, the amplitudes of the transmitted waves in the form

$$\begin{pmatrix}t_X\\ t_B\end{pmatrix} = \begin{pmatrix}\psi^+_X(+x_0)\\ \psi^+_B(+x_0)\end{pmatrix}. \quad (30)$$

The fields $\psi^-_{X,B}(x)$ are recovered from the known functions $\psi^+_{X,B}(x)$ and $\hat{R}(x)$ using Eq. (23).

As a result, we consecutively solve two evolutionary problems and determine the field distributions in the cyclotron region and, consequently, the amplitudes of the transmitted and reflected waves.

## 4. NUMERICAL SIMULATION RESULTS

For the above-described method of solving the wave equations to be applied, it is necessary to specify the parameters of the medium so that the condition of its homogeneity can be fulfilled outside the region $-x_0 < x < x_0$. For this, we specified the model profile of the magnetic field amplitude

$$\frac{2\omega_c}{\omega} = 1 + \delta \tanh\frac{x}{\delta L_B}. \quad (31)$$

Here, the multiplier 2 takes into account the number of the considered cyclotron harmonic. The technical parameters $x_0$ and $\delta$ were chosen so that the following inequalities were true

$$\max(2\pi/k_0, L_{res}) \ll \delta L_B \ll x_0. \quad (32)$$

Separately, we verified that the results of numerical calculations are independent of the values of the technical parameters, provided that those are chosen taking into account the described conditions.

In our problem, there are three physical parameters on which the coefficients of reflection, transmission and absorption depend. These are the ratio of plasma density to the critical value $\omega_p^2/\omega^2$, the ratio of the characteristic scale of the magnetic field inhomogeneity to the wavelength $k_0L_B$, and the ratio of the electron temperature to the rest energy of the electron $\mu^{-1} = T_e/mc^2$. Due to the resonance dependence of the dielectric response of the magnetic field, one can expect that the last two parameters will only be included in a combination [5]

$$\kappa = k_0L_B/\mu \approx k_0L_{res}, \quad (33)$$

which has a clear physical meaning: it is the ratio of the characteristic scale of the resonance region determined by Eq. (1) and the wavelength.

Equations (24) with initial conditions $\hat{R}(x_0) = 0$ and (28) were solved numerically by the Runge–Kutta method of the 4th order in the Python programming environment (the scipy.integrate library, RK45() function with default settings).

Figure 3 shows two examples of the calculated distributions of the electric field components inside the interaction region. The example in panel 3a has the parameters characteristic of the experiments on the ECR heating of the plasma at the second harmonic of the extraordinary wave at the L-2M stellarator [17]. The calculated coefficient of reflection $R_X = 1.56 \times 10^{-3}$ is in good agreement with the experimental results, where the measured energy reflection coefficient was $R = (1.8 \pm 0.8) \times 10^{-3}$ [17]. At the same time, the coefficient of reflection into the Bernstein wave was one order of magnitude smaller, $R_B = 0.12 \times 10^{-3}$. Since both reflection coefficients are small, in this case, the field distributions appear simply as an elec-

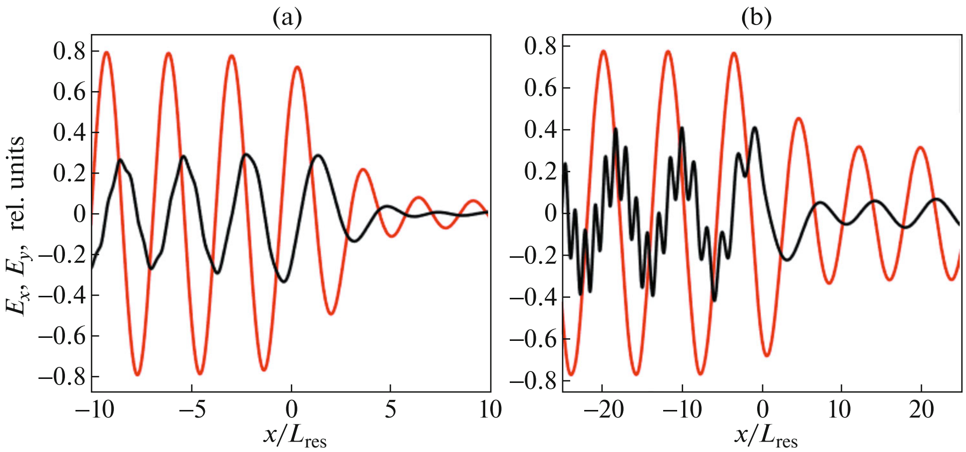


**Fig. 3.** Spatial distributions of the $E_x$ (black curves) and $E_y$ (red curves) components of the electric field (in relative units) inside the interaction region for $\omega_p^2/\omega^2 = 0.25$, $T_e = 1$ keV, and (a) $k_0L_B = 1354$ and (b) $k_0L_B = 511$.

tromagnetic wave with a changing amplitude that propagates left to right.

The example shown in Fig. 3b corresponds to a hypothetical case where the magnetic field changes in space approximately 3 times faster, which corresponds to $\kappa = 1$. It is seen that on a smaller scale of magnetic field inhomogeneity, the effects of the interaction between the electromagnetic and Bernstein waves are more pronounced. The linear transformation of the waves can be seen in the appearance of the short-wave modulation of the $E_x$ (longitudinal) component of the electric field. In this example, the coefficients of reflection into the extraordinary and Bernstein waves reach $R_X = 0.17$ and $R_B = 0.01$, respectively.

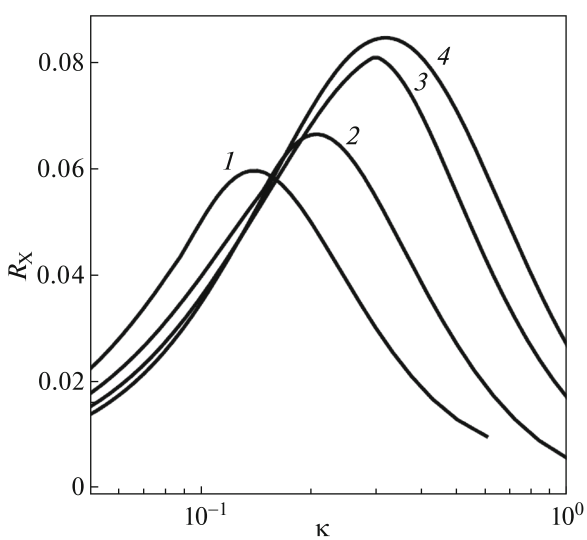


**Fig. 4.** Reflection coefficient into the extraordinary wave $R_X(\kappa)$ at (*1*) $k_0L_B = 3$, (*2*) $k_0L_B = 5$, (*3*) $k_0L_B = 10$, and (*4*) $k_0L_B = 50–1000$.

To illustrate the statement about the dependence of the reflection coefficients on a single parameter κ, Fig. 4 shows the dependences of the reflection coefficient into the extraordinary wave $R_X$ on this parameter at different scales of magnetic field inhomogeneity. It is seen that our assumption is confirmed by the numerical simulation results: while the inequality $k_0L_B > 50$ is true, the coefficient of reflection at a given plasma density is determined only by the parameter κ. The maximum reflection coefficient into the extraordinary wave is reached at $\varkappa \approx 0.3$, which corresponds to the characteristic width of the resonance region of the order of the wavelength of the electromagnetic radiation. At smaller sizes of the resonance region, the reflection coefficient decreases because the reflected wave does not have the chance to form in the resonance region if the latter is smaller than the wavelength.

Figure 5 shows the dependences of the reflection coefficients into the extraordinary $R_X$ and Bernstein $R_B$ waves on the parameter κ at different values of the dimensionless plasma density. These dependences were constructed for a specific value $\mu = 511$, but, as was shown above, they change weakly when this parameter (the electron temperatures) is varied. Therefore, they can be considered universal and describing all cases.

It is seen that the coefficient of reflection into the extraordinary wave changes with density almost by the automodel law. This is explained by the shift in the position of the maximum connected to the change in the real part of the refraction index of the extraordinary wave being small. Using the numerical simula-

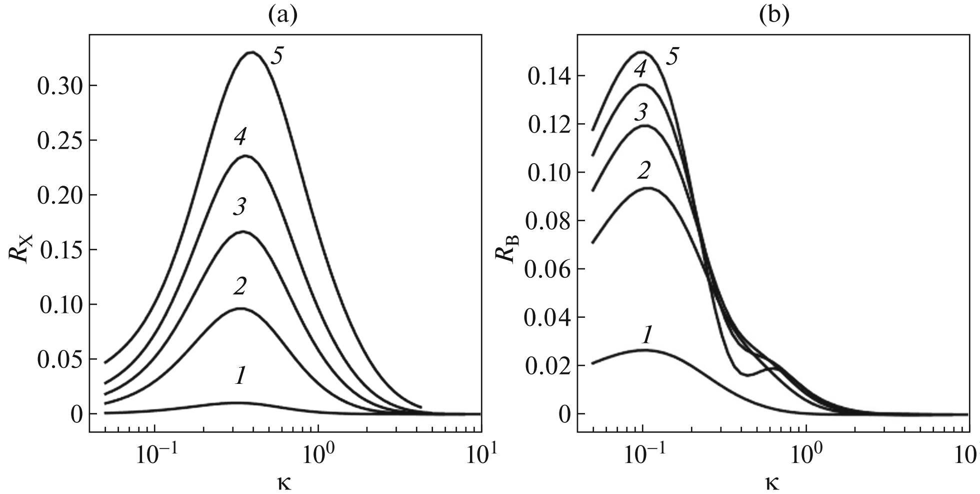


**Fig. 5.** Reflection coefficients into the (a) extraordinary and (b) Bernstein waves depending on κ for different values of the dimensionless plasma density: (*1*) $\omega_p^2/\omega^2 = 0.09$, (*2*) $\omega_p^2/\omega^2 = 0.25$, (*3*) $\omega_p^2/\omega^2 = 0.314$, (*4*) $\omega_p^2/\omega^2 = 0.36$, and (*5*) $\omega_p^2/\omega^2 = 0.41$. All curves were constructed for $T_e = 1$ keV.

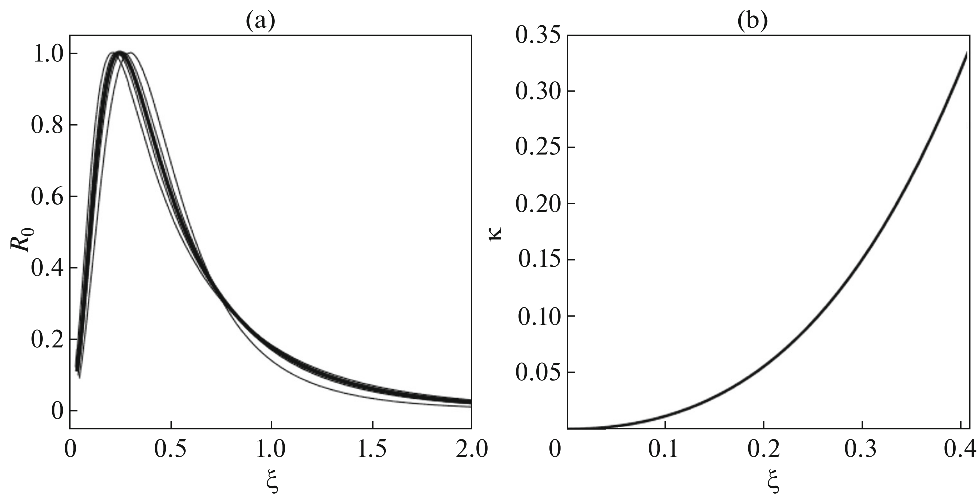


**Fig. 6.** $R_0(\xi)$ and $K(\xi)$ functions used in the approximation formula (34). In the figure, the bold curve represents $R_0(\xi)$ and the thin curves are the results of numerical simulations with different parameters that illustrate the error of the approximation formula.

tion results, one can propose a relatively simple approximate expression for the reflection coefficient

$$R_X \approx K(\omega_p^2/\omega^2) R_0(n_{X0}\kappa), \quad (34)$$

where

$$n_{X0}^2 = \left.\frac{2\varepsilon_+\varepsilon_-}{\varepsilon_+ + \varepsilon_-}\right|_{2\omega_c=\omega} = \frac{3 - 8\omega_p^2/\omega^2 + 4\omega_p^4/\omega^4}{3 - 4\omega_p^2/\omega^2} \quad (35)$$

is the nonperturbed (without taking thermal effects into account) refraction index of the extraordinary wave [16], and the one-dimensional functions $K(\xi)$ and $R_0(\xi)$ are determined numerically by fitting to the results of the precise calculation $R_X(\kappa, \omega_p/\omega)$. The tabulated functions $K(\xi)$ and $R_0(\xi)$ are shown in Fig. 6. The maximum error of the approximate formula (34) is less than 5% for the data presented in Fig. 5a.

The behavior of the coefficient of reflection into the Bernstein wave is significantly more complicated, see Fig. 5b. It is seen that, at low concentrations, the maximum of the reflection coefficient corresponds to $\kappa \approx 0.03$, and such a shift compared to the reflection coefficient into the extraordinary wave is connected to the high refraction index of the Bernstein wave. At

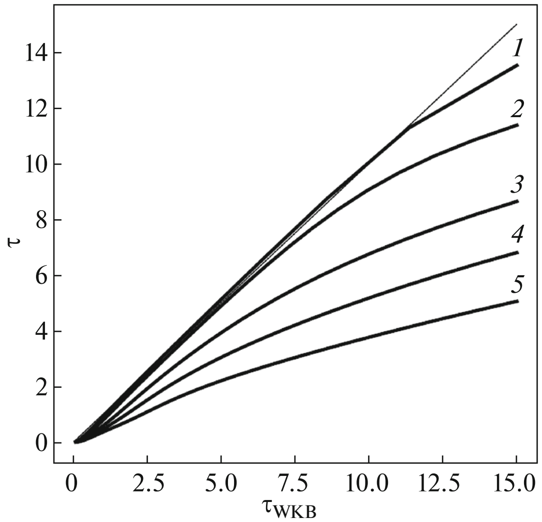


**Fig. 7.** Comparison between the "precise" optical thickness $\tau$ of the plasma layer relative to absorption calculated by solving Maxwell's equations numerically and the standard analytical estimate $\tau_{WKB}$ obtained in the framework of the WKB approximation. Curves *1*–*5* were calculated for the same values of plasma density as those used in Fig. 5 and the thin straight line corresponds to the WKB limit $\tau = \tau_{WKB}$.

high densities, when the maximum value of the reflection coefficient into the extraordinary wave exceeds 10%, a dip appears in the dependence of the reflection coefficient into the Bernstein wave in the region of parameters that correspond to the maximum reflection into the extraordinary wave.

Note that the fraction of processes connected to the reflection from the ECR region is not very large in the total energy balance of a hot plasma. In the parameter regions relevant for a sufficiently hot plasma in modern magnetic traps, the coefficient of reflection into the Bernstein wave is at least one order of magnitude lower than the coefficient of reflection into the extraordinary wave. However, at the initial stage of the discharge, when the plasma temperature is not yet very high, the reflection coefficient can be in the range of tens percent, and in this region, the reflection into the Bernstein wave can play an important role.

To illustrate the corrections to the total energy balance caused by reflection, Fig. 7 shows a comparison between the total optical thickness of the plasma layer by absorption calculated by the standard WKB formula without taking into account the reflection and the linear interaction and the one calculated by our method. The optical thickness $\tau$ is defined as

$$A = 1 - \exp(-\tau), \tag{36}$$

where $A$ is the coefficient of absorption of incident radiation determined by Eq. (18). In the WKB approximation, analytical expressions are known for the optical thickness (see, e.g., [9] and references therein), and, in particular, for the extraordinary wave at the second cyclotron harmonic

$$\tau_{WKB} = 2\pi \frac{\omega_p^2}{\omega^2}\left(\frac{3 - 2\,\omega_p^2/\omega^2}{3 - 4\,\omega_p^2/\omega^2}\right)^2 \times \sqrt{\frac{3 - 8\,\omega_p^2/\omega^2 + 4\omega_p^4/\omega^4}{3 - 4\,\omega_p^2/\omega^2}}\kappa. \tag{37}$$

Figure 7 shows that, although the analytical formula (37) provides a tolerable approximation of the optical thickness in the entire range of the simulation parameters, the deviation from the predictions of the standard theory constructed as the perturbation theory to the full set of Maxwell's equations can be quite substantial in a sufficiently dense plasma.

## 5. CONCLUSIONS

As a result of full-wave simulations taking into account the correct boundary conditions for the reflection of the extraordinary wave from the cyclotron resonance region at the second harmonic in a hot magnetoactive plasma, the coefficients of reflection, linear transformation, transmission, and absorption of the extraordinary wave were analyzed. The simulations were in good agreement with the experimental results obtained at the L-2M stellarator. It was shown that, at the stage of the temperature rise, the coefficient of reflection of the electromagnetic radiation can reach tens of percent.

## FUNDING

This work was carried out under the State Assignment of the Gaponov-Grekhov Institute of Applied Physics, Russian Academy of Sciences (IAP RAS) (project no. FFUF-2023-0002) and the Ioffe Institute, Russian Academy of Sciences (II RAS) (according to the contract between IAP RAS and II RAS no. OK44-2-21 from August 6, 2021).

## CONFLICT OF INTEREST

The authors declare that they have no conflicts of interest.

## REFERENCES


1. A. V. Timofeev, *Resonance Phenomena in Plasma Oscillations,* 1st and 2nd eds. (Fizmatlit, Moscow, 2000 and 2009) [in Russian].
2. V. I. Fedorov, Sov. Tech. Phys. Lett. **6**, 560 (1980).
3. M. Bornatici, F. Engelmann, C. Maroli, and V. Petrillo, Plasma Phys. **23**, 89 (1981).
4. E. Lazzaro, G. Ramponi, and G. Giruzzi, Phys. Fluids **25**, 1220 (1982).
5. A. V. Zvonkov, Sov. J. Plasma Phys. **9**, 319 (1983).
6. A. V. Timofeev, Sov. Phys.—Usp. **16**, 445 (1974).
7. I. B. Bernstein, Phys. Rev. **109**, 10 (1958).
8. A. G. Litvak, E. V. Suvorov, G. V. Permitin, and A. A. Fraiman, Nucl. Fusion **17**, 659 (1977).
9. V. V. Alikaev, A. G. Litvak, E. V. Suvorov, and A. A. Fraiman, in *High-Frequency Plasma Heating,* Ed. by A. G. Litvak (AIP, New York, 1992), p. 1.
10. M. Tereshchenko, F. Castejón, and A. Cappa, Informes Técnicos CIEMAT No. 1134 (CIEMAT, Madrid, 2008).
11. R. Prater, D. Farina, Yu. Gribov, R. W. Harvey, A. K. Ram, Y.-R. Lin-Liu, E. Poli, A. P. Smirnov, F. Volpe, E. Westerhof, A. Zvonkov, and the ITPA Steady State Operation Topical Group, Nucl. Fusion **48**, 035006 (2008).
12. G. V. Pereverzev, Phys. Plasmas **5**, 3529 (1998).
13. A. A. Balakin, M. A. Balakina, and E. Westerhof, Nucl. Fusion **48**, 065003 (2008).
14. A. A. Balakin, Radiophys. Quantum Electron. **55**, 502 (2012).
15. A. G. Shalashov, A. A. Balakin, E. D. Gospodchikov, and T. A. Khusainov, Phys. Plasmas **23**, 112504 (2016).
16. V. L. Ginzburg, *The Propagation of Electromagnetic Waves in Plasmas* (Nauka, Moscow, 1967; Pergamon, Oxford, 1970).
17. G. M. Batanov, V. D. Borzosekov, L. V. Kolik, E. M. Konchenkov, D. V. Malakhov, A. E. Petrov, K. A. Sarksyan, A. S. Sakharov, N. N. Skvortsova, V. D. Stepakhin, and N. K. Kharchev, Plasma Phys. Rep. **39**, 882 (2013).
18. E. Westerhof, S. K. Nielsen, J. W. Oosterbeek, M. Salewski, M. R. De Baar, W. A. Bongers, A. Bürger, B. A. Hennen, S. B. Korsholm, F. Leipold, D. Moseev, M. Stejner, and D. J. Thoen (the TEXTOR Team), Phys. Rev. Lett. **103**, 125001 (2009).
19. S. K. Nielsen, M. Salewski, E. Westerhof, W. Bongers, S. B. Korsholm, F. Leipold, J. W. Oosterbeek, D. Moseev, M. Stejner, and the TEXTOR Team, Plasma Phys. Controlled Fusion **55**, 115003 (2013).
20. S. K. Hansen, S. K. Nielsen, J. Stober, J. Rasmussen, M. Stejner, M. Hoelzl, T. Jensen, and the ASDEX Upgrade team, Nucl. Fusion **60**, 106008 (2020).
21. A. S. Sakharov, Plasma Phys. Rep. **43**, 1065 (2017).
22. A. G. Shalashov and E. D. Gospodchikov, Phys.—Usp. **54**, 145 (2011).
23. A. G. Shalashov and E. D. Gospodchikov, Plasma Phys. Controlled Fusion **52**, 025007 (2010).
24. M. R. Scott, *Invariant Imbedding and Its Applications to Ordinary Differential Equations: an Introduction* (Addison-Wesley, London, 1973).
25. V. I. Klyatskin, *Immersion Method in Wave Propagation Theory* (Nauka, Moscow, 1986) [in Russian].
26. Yu. N. Dnestrovskii, D. P. Kostomarov, and N. V. Skrydlov, Sov. Phys.—Tech. Phys. **8**, 691 (1964).
27. V. D. Shafranov, in *Reviews of Plasma Physics,* Ed. by M. A. Leontovich (Consultants Bureau, New York, 1967), Vol. 3, p. 1.


*Translated by E. Voronova*